A&A 464, 277–287 (2007)
DOI: 10.1051/0004-6361:20066517

Astronomy & Astrophysics

X-ray broad-band study of the symbiotic X-ray binary 4U 1954+31⋆

N. Masetti[1], E. Rigon[2], E. Maiorano[1,3], G. Cusumano[4], E. Palazzi[1], M. Orlandini[1], L. Amati[1], and F. Frontera[1,3]

[1] INAF – Istituto di Astrofisica Spaziale e Fisica Cosmica di Bologna, via Gobetti 101, 40129 Bologna, Italy
(formerly IASF/CNR, Bologna)
e-mail: masetti@iasfbo.inaf.it
[2] Dipartimento di Fisica, Università di Bologna, via Irnerio 48, 40126 Bologna, Italy
[3] Dipartimento di Fisica, Università di Ferrara, via Saragat 1, 44100 Ferrara, Italy
[4] INAF – Istituto di Astrofisica Spaziale e Fisica Cosmica di Palermo, Via Ugo La Malfa 153, 90146 Palermo, Italy
(formerly IASF/CNR, Palermo)

Received 6 October 2006 / Accepted 14 November 2006

ABSTRACT

We present results of several pointed X-ray broad band observations of the "symbiotic X-ray binary" 4U 1954+31 performed with the satellites *BeppoSAX*, *EXOSAT*, *ROSAT*, *RXTE* and *Swift* between October 1983 and April 2006. We also studied the *RXTE* ASM data over a period of more than 10 years, from January 1996 to October 2006. Light curves of all pointed observations show an erratic behaviour with sudden increases in the source emission on timescales variable from hundreds to thousands of seconds. There are no indications of changes in the source spectral hardness, with the possible exception of the *RXTE* pointed observation. Timing analysis does not reveal the presence of coherent pulsations or periodicities either in the pointed observations in the range from 2 ms to 2000 s or in the long-term *RXTE* ASM light curve on timescales from days to years. The 0.2−150 keV spectrum, obtained with *BeppoSAX*, is the widest for this source available to date in terms of spectral coverage and is well described by a model consisting of a lower-energy thermal component (hot diffuse gas) plus a higher-energy (Comptonization) emission, with the latter modified by a partially-covering cold absorber plus a warm (ionized) absorber. A blackbody modelization of our *BeppoSAX* low-energy data is ruled out. The presence of a complex absorber local to the source is also supported by the 0.1−2 keV *ROSAT* spectrum. *RXTE*, *EXOSAT* and *Swift* X-ray spectroscopy is consistent with the above results, but indicates variations in the density and the ionization of the local absorber. A 6.5 keV iron emission line is possibly detected in the *BeppoSAX* and *RXTE* spectra. All this information suggests that the scenario that better describes 4U 1954+31 consists of a binary system in which a neutron star orbits in a highly inhomogeneus medium, accreting matter from a stellar wind coming from its optical companion, an M-type giant star.

Key words. stars: binaries: close – X-rays: binaries – stars: individual: 4U 1954+31 – stars: neutron – accretion, accretion disks

1. Introduction

X-ray binaries are interacting systems composed of a compact object, neutron star (NS) or black hole (BH), which accretes matter from a "normal" star orbiting at close distance. According to the mass of the donor star, these systems are classified as High Mass X-Ray Binaries (HMXBs) or Low Mass X-ray Binaries (LMXBs). Among LMXBs, the mass transfer generally occurs through inner Lagrangian point matter overflow from a Roche Lobe filling red dwarf (e.g., White et al. 1995; van Paradijs & McClintock 1995).

However, there exists a very small subclass of LMXBs (3 out of more than 150 objects: Liu et al. 2001; Masetti et al. 2006a) that host an M-type giant mass-losing star. This red giant is believed to feed the compact companion via its stellar wind. By analogy with the symbiotic stars, which are systems composed of an M-type giant and a white dwarf (WD), these LMXBs are sometimes referred to as "symbiotic X-ray binaries". The prototype of this small subclass, the system GX 1+4, is a well-studied case (e.g., Chakrabarty & Roche 1997); the second member, object 4U 1700+24, is now receiving more attention (Masetti et al. 2002, 2006a; Galloway et al. 2002; Tiengo et al. 2005).

The third member of this class, 4U 1954+31, despite being relatively luminous in X-rays (it is an *Uhuru* source), has been neglected over the years. The object was first detected in the '70s in this spectral window by *Uhuru* (Forman et al. 1978) and subsequently by *Ariel V* (Warwick et al. 1981) in the framework of their all-sky surveys. Warwick et al. (1981) found the source at an average flux of $\approx 2 \times 10^{-10}$ erg cm^{-2} s^{-1} in the 2−10 keV band, with long-term variability of a factor of more than 20.

The first pointed observation was performed with *EXOSAT* in October 1983. The data (Cook et al. 1984) showed flaring behavior on 1−10 min timescales but no evidence of pulsations or periodic variations; the 1−20 keV spectrum was modeled with either a powerlaw with photon index $\Gamma \sim 1.5$ or a bremsstrahlung model with $kT \sim 36$ keV. These characteristics led Cook et al. (1984) to conclude that 4U 1954+31 is probably an HMXB hosting a compact object accreting from a highly inhomogeneous wind from a companion star of early spectral type.

Subsequently, 4U 1954+31 was observed in October 1987 by *Ginga* in the 2−30 keV band (Tweedy et al. 1989). This observation confirmed the timing characteristics found by Cook et al. (1984) and allowed Tweedy et al. (1989) to model the spectrum of the source with a high-energy cutoff powerlaw plus

⋆ Appendix is only available in electronic form at
http://www.aanda.org

a soft excess below 4 keV, heavily absorbed by intervening matter (possibly local to the source) partially covering the soft X-ray emission. These authors also found spectral variability which they interpreted as due to changes in both the continuum shape and the absorption column. Tweedy et al. (1989) also (unsuccessfully) searched for the optical counterpart of this source, concluding that the M-type giant within the *EXOSAT* error circle is unlikely associated with 4U 1954+31 and that the true counterpart should be an H_α-emitting, highly reddened object (most likely a supergiant secondary hosted in an HMXB).

Notwithstanding all of the above, which makes 4U 1954+31 a potentially interesting target for X-ray studies, no refereed publications were devoted to this source, and no optical counterpart has been associated with it, up to March 2006. After a hiatus of nearly 20 years, Masetti et al. (2006a), thanks to a pointed *Chandra* observation and a spectroscopic optical follow-up, showed that the M-type giant mentioned above is indeed the optical counterpart of 4U 1954+31, and that this system is a symbiotic X-ray binary located at a distance $d \lesssim 1.7$ kpc.

The work of Masetti et al. (2006a) shed light on this high-energy emitting source, and revived the interest in this object: a fast flare (lasting less than 2 h) from 4U 1954+31 was detected with *INTEGRAL* in April 2006 and was communicated by Paltani et al. (2006); also, Corbet et al. (2006) found a 5-h periodic modulation in the *Swift* BAT data acquired between December 2004 and September 2005. Mattana et al. (2006), using *INTEGRAL* observations and a subset of the data presented in this work, confirmed the NS spin period and the high absorption in the X-ray spectrum.

In the present paper, we collect all of the unpublished archival X-ray observations on this system to fully characterize its high-energy behaviour and characteristics in both temporal (long- and short-term) and spectral scales. Particular attention is paid to the still unexplored parts of the X-ray spectrum of 4U 1954+31, i.e. below 2 keV and above 30 keV, where the high sensitivity of *BeppoSAX* is of paramount importance to gauge the source emission.

The aim of this paper is therefore to study the high energy properties of 4U 1954+31, and in particular the soft excess seen by Tweedy et al. (1989) below 4 keV. With this purpose, we have analyzed the data collected on 4U 1954+31 obtained over a time span of ∼23 years through pointed observations performed with various satellites (*EXOSAT*, *ROSAT*, *RXTE*, *Swift* and *BeppoSAX*). We have also retrived the data collected with the *RXTE* All-Sky Monitor (ASM), in order to have a better view of the source long-term X-ray activity.

2. Observations and data reduction

Here we describe the X-ray observations of 4U 1954+31 made with five different spacecraft. Table 1 reports the log of all the X-ray pointed observations presented in this paper.

2.1. *BeppoSAX* data

This source was observed with the Narrow Field Instruments (NFIs) onboard *BeppoSAX* (Boella et al. 1997a) on 4 May 1998. The NFIs included the Low-Energy Concentrator Spectrometer (LECS, 0.1−10 keV; Parmar et al. 1997), two Medium-Energy Concentrator Spectrometers (MECS, 1.5−10 keV; Boella et al. 1997b), a High Pressure Gas Scintillation Proportional Counter (HPGSPC, 4−120 keV; Manzo et al. 1997), and the Phoswich Detection System (PDS, 15−300 keV; Frontera et al. 1997).

Table 1. Log of the X-ray pointings on 4U 1954+31 analyzed in this paper.

Satellite	Obs. start date	Obs. start time (UT)	Exposure (ks)	On-source time (ks)
EXOSAT	22 Oct. 1983	21:50:00	15.2	14.7 (GSPC)
		21:53:04	14.8	13.4 (ME)*
	02 Jun. 1985	06:54:08	16.3	14.8 (GSPC)
		06:57:20	5.3	5.2 (ME)
		08:37:36	10.2	8.9 (ME)
ROSAT	04 May 1993	12:28:52	98.1	7.9 (PSPC B)
RXTE	14 Dec. 1997	03:44:11	15.0	8.4 (PCA)
		03:44:11	15.0	2.6 (HEXTE)
BeppoSAX	04 May 1998	22:05:14	92.4	20.0 (LECS)
		22:05:14	92.4	46.4 (MECS)
		22:05:14	92.4	20.0 (HPGSPC)
		22:05:14	92.4	21.0 (PDS)
Swift	19 Apr. 2006	21:02:10	7.1	2.5 (XRT)

* Results from this observation were partially presented by Cook et al. (1984).

LECS and MECS were imaging instruments, whereas HPGSPC and PDS were non-imaging collimated detectors with fields of view of about 1.°0 and 1.°3, respectively. During all pointings the four NFIs worked nominally and the source was detected by all of them.

Good NFI data were selected from intervals outside the South Atlantic Geomagnetic Anomaly when the elevation angle above the earth limb was >5°, when the instrument functioning was nominal and, for LECS events, during spacecraft night time. The SAXDAS 2.0.0 data analysis package (Lammers 1997) was used for the extraction and the processing of LECS, MECS and HPGSPC data. The PDS data reduction was instead performed using XAS version 2.1 (Chiappetti & Dal Fiume 1997). LECS and MECS data were reduced using an extraction radius of 4′, centered on the source position; before extraction, data from the two MECS units were merged.

Background subtraction for the two imaging instruments was performed using standard library files, while the background for the PDS data was evaluated from two fields observed during off-source pointing intervals. Due to the presence of the strong X-ray source Cyg X-1 in one of the off-source pointings, only the other one was used for the background subtraction. For the same reason, the background for the HPGSPC data was computed through an Earth-occultation technique (Manzo et al. 1997).

Inspection of the MECS data shows the presence of a field X-ray source, located at ∼21′ from 4U 1954+31, which we identify with the dwarf nova EY Cyg. By studying its X-ray spectrum (see Appendix) and extrapolating it to the ranges covered by the non-imaging instruments HPGSPC and PDS, we could determine the degree of contamination of the X-ray emission of this source on the hard X-ray spectrum of 4U 1954+31. It is found that the X-ray emission of EY Cyg is less than 0.1% of the flux detected from 4U 1954+31 above 7 keV (see Sect. 3.2), thus negligible. No contamination from EY Cyg is present in the MECS data because it appears fully separated from 4U 1954+31 in the observation acquired by this imaging instrument. EY Cyg was not observed by the LECS as it was outside its field of view.

We also checked for the presence of other contaminating X-ray sources in the PDS and HPGSPC fields of view. Only three *ROSAT* sources (Voges et al. 1999, 2000) were found at the edge of the PDS field of view, at distances of more than 35′ from 4U 1954+31. Assuming conservatively a hard spectral photon index $\Gamma = 1$ for all of them, we determined their total flux

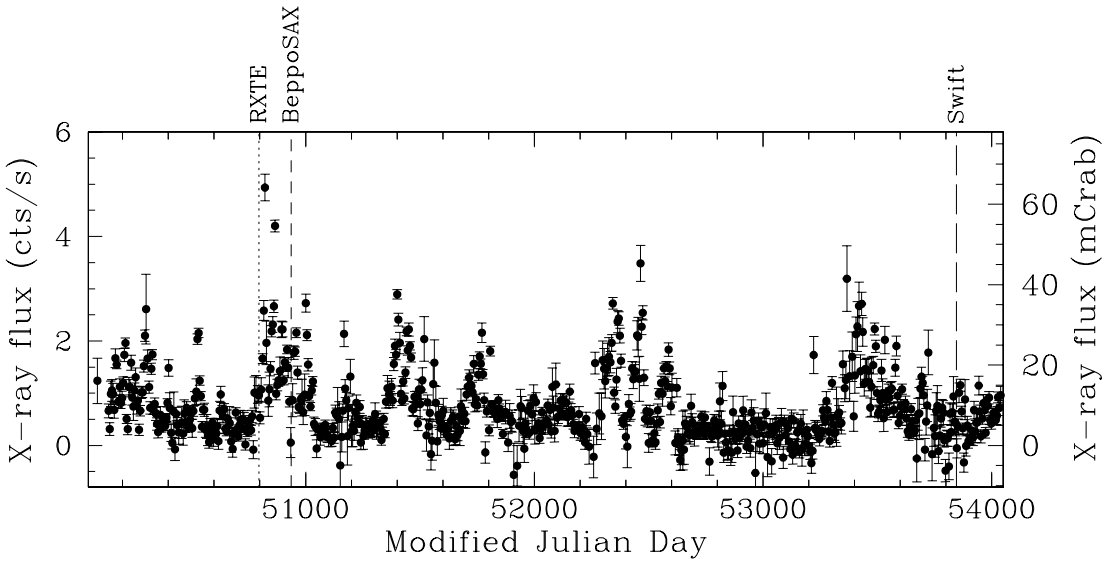

Fig. 1. 1.5−12 keV 5–day averaged *RXTE* ASM light curve of 4U 1954+31. One ASM count s^{-1} roughly corresponds to 13 mCrab assuming a Crab-like spectrum. In the plot the times of the pointed *RXTE*, *BeppoSAX* and *Swift* are indicated by the vertical dashed lines (different dashes correspond to different spacecraft). A series of aperiodic increases in the X-ray activity from the source are noticed occurring on timescales variable from 200 to 400 days.

convolved with the PDS triangular response. We found that their contamination in the 15−150 keV band is less than 0.9% of the flux of 4U 1954+31 in this band (see Sect. 3.2), and therefore negligible as well.

In the same way, we evaluated the contamination of field X-ray sources on the PDS background measurement: 5 *ROSAT* sources were found in the off-source field used for background evaluation; it is found that these contribute less than 0.35% of the total measured background. Thus, again in this case, we can neglect this contribution.

2.2. Other public X-ray data

In order to present a thorough long-term analysis of the X-ray behaviour of 4U 1954+31, we also retrieved from the HEASARC archive[1] all the unpublished X-ray observations of this source. These include (see Table 1) *ROSAT*, *RXTE*, *EXOSAT* and *Swift* data; we also re-examine the *EXOSAT* pointing already partially studied by Cook et al. (1984).

Two pointed observations were performed on 4U 1954+31 with the *EXOSAT* satellite (White & Peacock 1988). The first one (*EXOSAT* I) was acquired on 22 October 1983 while the second one (*EXOSAT* II) on 2 June 1985. Both observations were made using the Medium Energy (ME; Turner et al. 1981) proportional counter, in the 1−50 keV band, and with the Gas Scintillation Proportional Counter (GSPC; Peacock et al. 1981), in the range 2−20 keV. However, due to their very low signal-to-noise ratio (S/N), GSPC data of *EXOSAT* II were not used in this analysis.

The *ROSAT* satellite (Trümper 1982) was pointed at 4U 1954+31 on 4 May 1993 with the Position Sensitive Proportional Counter (PSPC; Pfeffermann & Briel 1986) unit B, sensitive in the 0.1−2.4 keV range.

The *RXTE* satellite (Bradt et al. 1993) observed the source on 14 December 1997; this satellite carries a 5-unit Proportional Counter Array (PCA; Jahoda et al. 1996), which is sensitive in the 2−60 keV energy range and allows a time resolution of 1 μs, and a High Energy X-ray Timing Experiment (HEXTE; Rothschild et al. 1998) composed of two clusters of 4 phoswich scintillation detectors working in the 15−250 keV band.

This satellite also carries an ASM[2] (Levine et al. 1996) which regularly scans the X-ray sky in the 1.5−12 keV range with a daily sensitivity of 5 mCrab. Figure 1 reports the complete 1.5−12 keV ASM light curve of 4U 1954+31 starting on January 1996 up to October 2006, along with the times of the *BeppoSAX*, *RXTE* and *Swift* pointed observations. In order to clearly display the long-term trend in the X-ray emission from 4U 1954+31, each point in Fig. 1 is computed as the average of 5 subsequent measurements; given that the single original ASM points we retrived were acquired on a daily basis (i.e. they are one-day averaged measurements), the plot illustrated in Fig. 1 corresponds to a 5-day averaged X-ray light curve.

Further X-ray data of 4U 1954+31 were collected on 19 April 2006 with the X-Ray Telescope (XRT, 0.2−10 keV; Burrows et al. 2006) on board *Swift* (Gehrels et al. 2004). The data reduction was performed using the XRTDAS v2.4 standard data pipeline package (`xrtpipeline` v0.10.3), in order to produce the final cleaned event files.

As the XRT count rate of the source was high enough to cause pile-up in the data, we extracted the source events in an annulus, of 12″ inner radius and 45″ outer radius, centered on the source. The size of the inner region was determined following the procedure described in Romano et al. (2006). The source background was measured within a circle with radius 80″ located far from the source. The ancillary response file was generated with the task `xrtmkarf` (v0.5.2) within FTOOLS[3] (Blackburn 1995), and accounts for both extraction region and PSF pile-up correction. We used the latest spectral redistribution

[1] Available at: `http://heasarc.gsfc.nasa.gov/cgi-bin/W3Browse/w3browse.pl`

[2] ASM light curves are available at: `http://xte.mit.edu/ASM_lc.html`

[3] Available at: `http://heasarc.gsfc.nasa.gov/ftools/`

matrices in the Calibration Database[4] (CALDB 2.3) maintained by HEASARC.

We determined the source position using the `xrtcentroid` (v0.2.7) task. The correction for the misalignment between the telescope and the satellite optical axis was taken into account (see Moretti et al. 2006 for details). The *Swift* XRT position we obtained for 4U1954+31 is the following (J2000): RA = $19^{\rm h}55^{\rm m}42\overset{\rm s}{.}28$; Dec = $+32^{\circ}05'45\overset{''}{.}5$ (with a 90% confidence level error of $3\overset{''}{.}6$ on both coordinates).

These coordinates are consistent with the (more accurate) ones measured in X-rays with *Chandra* and with those of the optical counterpart (Masetti et al. 2006a). We remark that the uncertainty in the source coordinates as determined with the *Swift* XRT data may be underestimated because, as said above, the XRT observation is affected by pile-up and the PSF of the source image is thereby distorted.

3. Results

3.1. Light curves and timing analysis

The *RXTE* long-term (January 1996/October 2006) 1.5−12 keV ASM light curve (see Fig. 1) of 4U 1954+31 shows an erratic behaviour of the source with sudden increases in its activity. The timing analysis of the 5-day averaged data has not revealed a coherent periodicity but only a variability on timescales between 200 and 400 days. A similar indication is obtained using the dwell-by-dwell and the daily-averaged ASM data sets.

We also studied the short-term X-ray light curves obtained with the pointed observations on 4U 1954+31 (see Fig. 2). The light curves have different bin times (from 50 s to 300 s) depending on their S/N.

All light curves show an erratic flaring activity on timescales variable between 100 s and 1000 s, the longer ones corresponding to the more intense flares. In particular, *EXOSAT* I shows the most intense flaring activity among the observations presented here, while during *EXOSAT* II the source was more active in the first part of the observation.

As Cook et al. (1984) and Tweedy et al. (1989) pointed out some variability in the source hardness ratio as a function of the X-ray count rate, we investigated the presence of this possible correlation for 4U 1954+31. However, we did not find any change in the spectral hardness with X-ray intensity in any observation. Only *RXTE* data suggest a slight hardening with increased source intensity.

Timing analysis on the X-ray light curves from the various spacecraft was performed with the FTOOLS task XRONOS, version 5.21, after having converted the event arrival times to the solar system barycentric frame. The data were searched for coherent pulsations or periodicities but no evidence for them was found in the range 2 ms to 2000 s, although above 10 s any coherent behaviour could be significantly masked by the flaring activity of 4U 1954+31 (see Fig. 2). The power spectral densities obtained for each pointing are characterized by red noise and show no significant deviation from the $1/f$-type distribution (where f is the time frequency) typical of the "shot-noise" behaviour.

Likewise, a Fast Fourier Transform (FFT) analysis was made to search for fast periodicities (pulsations or QPOs) in the 1−2000 Hz range within the *RXTE* PCA data. During the observation, data in "Good Xenon" mode with a 2^{-20} s (i.e. 1 μs) time resolution and 256 energy bands were available. To search for fast pulsations and/or kiloHertz QPOs we made several FFTs of 16 s long data segments in the 2−10 keV and 10−60 keV energy intervals and with a Nyquist frequency of 4096 Hz. We then calculated the Z^2 statistics (Buccheri et al. 1983) on each ∼3000 s long subinterval of the *RXTE* PCA observation (see Fig. 2, central left panel) and finally added together the results. No presence of QPO peaks or of coherent pulsations was detected.

3.2. Spectra

In order to perform spectral analysis, the pulse-height spectra from the detectors of all spacecraft were rebinned to oversample by a factor 3 the full width at half maximum of the energy resolution and to have a minimum of 20 counts per bin, such that the χ^2 statistics could reliably be used. For all detectors, data were then selected, when a sufficient number of counts were obtained, in the energy ranges where the instrument responses are well determined. In all cases we considered the average spectra of 4U 1954+31 given that no substantial variations in the spectral shape during each pointed observation were suggested by the inspection of the color-intensity diagram of the source (See Sect. 3.1).

Spectral analysis was performed with the package XSPEC (Arnaud 1996) v11.3.1. In the broad band *BeppoSAX* fits, normalization factors were applied to LECS, HPGSPC and PDS spectra following the cross-calibration tests between these instruments and the MECS: these factors were fixed to the best estimated values (Fiore et al. 1999). Similarly, a constant was introduced between HEXTE and PCA in the *RXTE* spectra as well as between ME and GSPC in the *EXOSAT* spectra to take the different instrumental sensitivities into account. The spectra from the two HEXTE clusters were fitted independently and the normalization between them was left free, because of the presence of a small systematic difference between their responses.

To all spectral models tested in this paper (the best-fit models for each satellite pointing are reported in Table 2), we applied a photoelectric absorption column, modeled using the cross sections of Morrison & McCammon (1983; WABS in XSPEC notation), to describe the line-of-sight Galactic neutral hydrogen absorption towards 4U 1954+31. In the following, the acronym "d.o.f." means "degrees of freedom". Table 3 reports values or 90% confidence level upper limits of the Equivalent Width (EW) of any Fe emission line at ∼6.5 keV in the spectrum of each pointed observation.

We first considered the 0.2−150 keV *BeppoSAX* spectrum as it is the one with the widest spectral coverage. The initial attempt to fit this spectrum with a simple model such as a power law was unsatisfactory and indicated the presence of a soft excess below ∼2 keV and of a spectral turnover above 20 keV. The use of single-component models therefore proved to be inadequate, giving unacceptable reduced χ^2 values (>3).

Mattana et al. (2006) described the X-ray spectrum of this source above 18 keV with a phenomenological model made of a cutoff power law. Our 15−150 keV PDS spectrum can be well fit with the same model and our results are compatible with theirs. When including the lower part of their broadband X-ray data, Mattana et al. (2006) used an absorbed cutoff power law plus blackbody model; however, they note that their spectral description is poor at low energies. We reached the same conclusion when applying this same model to our *BeppoSAX* spectrum, which means that a different and more physical modeling should be used.

[4] Available at: `http://heasarc.gsfc.nasa.gov/docs/heasarc/caldb/caldb_intro.html`

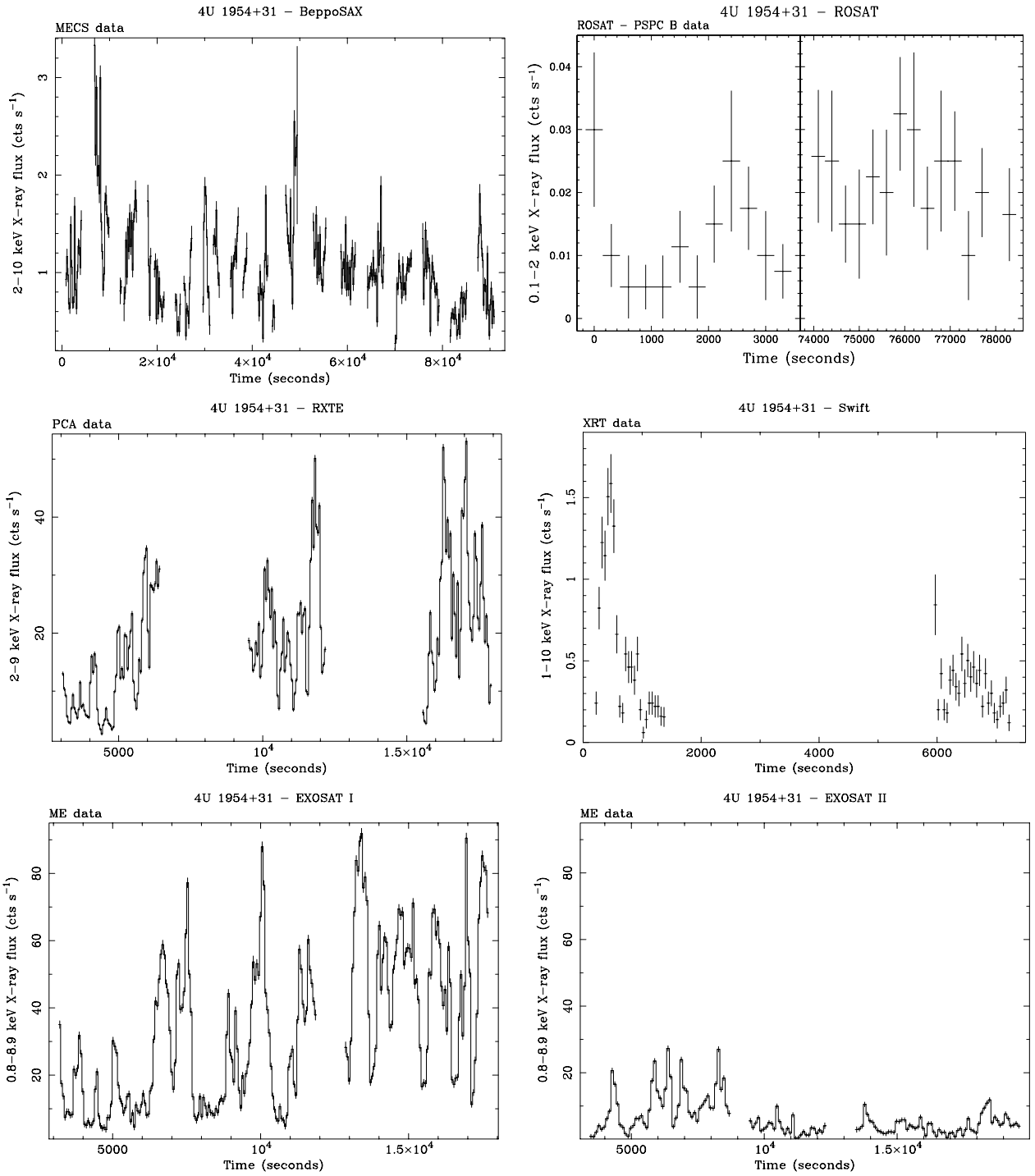

Fig. 2. Background-subtracted X-ray light curves of 4U 1954+31 as seen during the pointed observations reported in the text. (*Upper panels*) 2–10 keV light curve of *BeppoSAX* MECS (*left*) and 0.1–2 keV light curve of *ROSAT* PSPC B (*right*). The former is binned at 200 s, the latter at 300 s. (*Central panels*) 2–9 keV *RXTE* PCA (*left*) and 1–10 keV *Swift* XRT (*right*) light curves. Both light curves are binned at 50 s. (*Lower panels*) 0.8–8.9 keV light curves of *EXOSAT* ME observations I (*left*) and II (*right*). The former is binned at 60 s, the latter at 100 s; for the sake of comparison of the activity of the source between the two *EXOSAT* observations, the latter panels were plotted using the same *y*-axis scaling. Given that, during the *ROSAT* observation, good source events were recorded only at the beginning and at the end of the pointing, we plot here these two time intervals. In all figures, times are in seconds since the beginning of the observation as reported in Table 1.

We therefore assumed, as already applied to the X-ray spectra of this type of source (Masetti et al. 2002), a composite model made of a Comptonization component (COMPTT in XSPEC; Titarchuk 1994) and a thermal component to describe the emissions above and below 2 keV, respectively. We however found that, in order to describe the *BeppoSAX* spectrum at low energy, a complex absorption pattern was needed, with different absorption columns acting on the two components. In particular we found that, while on the thermal component a simple neutral hydrogen absorbing column was needed, a mixture of a partial

Table 2. Best-fit parameters for the X-ray spectra of 4U 1954+31 from the pointed observations described in this paper. In all models in which a Fe emission line is needed in the fit, its width is fixed at the value $\sigma = 0.1$ keV. Frozen parameters are written between square brackets. Luminosities are not corrected for the intervening absorptions and are computed assuming a distance $d = 1.7$ kpc (Masetti et al. 2006a); in the cases in which the X-ray data could not completely cover the X-ray interval of interest for the luminosity determination, an extrapolation of the best-fit model is applied. Errors are at 90% confidence level for a single parameter of interest. Observations are reported in chronological order from left to right.

model: WABS*[PCFABS*WNDABS(COMPTT + GAUSS) + MEKAL]						
Parameters[a]	*EXOSAT* I (1−15 keV)	*EXOSAT* II (1−15 keV)	*ROSAT* (0.1−2 keV)	*RXTE* (2.5−100 keV)	*BeppoSAX* (0.2−150 keV)	*Swift* (1.8−8.5 keV)
χ^2/d.o.f.	217.7/204	86.0/85	20.0/18	112.6/105	280.1/247	53.4/44
$N_{\rm H}^{\rm WABS}$	[1.5]	[1.5]	[1.5]	[1.5]	$1.5^{+0.6}_{-0.4}$	[1.5]
$N_{\rm H}^{\rm PCFABS}$	—	—	[25.4]	—	25.4 ± 1.6	$1.4^{+2.6}_{-1.2}$
$C_{\rm PCFABS}$ (%)	—	—	[95]	—	95 ± 2	[95]
$N_{\rm H}^{\rm WNDABS}$	—	—	[3.0]	$4.1^{+0.2}_{-0.3}$	$3.0^{+1.3}_{-0.7}$	—
$E_{\rm WNDABS}$ (keV)	—	—	[1.86]	[1.86]	$1.86^{+0.10}_{-0.13}$	—
kT_0 (keV)	0.56 ± 0.04	$0.94^{+0.05}_{-0.06}$	[1.28]	$1.156^{+0.017}_{-0.009}$	1.28 ± 0.06	$0.6^{+0.4}_{-0.6}$
$kT_{\rm e^-}$ (keV)	$2.86^{+0.12}_{-0.10}$	$13^{+\infty}_{-9}$	[9.9]	13^{+14}_{-3}	9.9 ± 0.8	$8^{+\infty}_{-2}$
τ	$9.4^{+0.5}_{-0.4}$	$3.2^{+2.5}_{-3.2}$	[2.8]	$2.0^{+0.5}_{-0.4}$	$2.8^{+0.3}_{-0.2}$	4^{+5}_{-4}
$K_{\rm COMPTT}$ ($\times 10^{-3}$)	50^{+2}_{-3}	$2.1^{+3.6}_{-2.1}$	[8.2]	$5.0^{+0.4}_{-2.4}$	8.2 ± 0.8	6^{+120}_{-6}
$kT_{\rm MEKAL}$ ($\times 10^{-2}$ keV)	—	—	$5.3^{+1.5}_{-1.2}$	—	$6.8^{+2.2}_{-1.5}$	—
$K_{\rm MEKAL}$	—	—	300^{+5600}_{-290}	—	200^{+5400}_{-190}	—
$E_{\rm Fe}$ (keV)	—	—	N/A	$6.46^{+0.12}_{-0.11}$	$6.46^{+0.10}_{-0.11}$	—
$I_{\rm Fe}$ ($\times 10^{-4}$ ph cm^{-2} s^{-1})	—	—	N/A	$1.9^{+0.5}_{-0.4}$	2.5 ± 1.0	—
X-ray luminosities[b]:						
0.1−2 keV	—	—	4.1×10^{31}	—	2.0×10^{32}	—
2−10 keV	1.8×10^{35}	3.4×10^{34}	—	7.9×10^{34}	5.2×10^{34}	5.2×10^{34}
10−100 keV	—	—	—	1.2×10^{35}	1.8×10^{35}	—

[a] Hydrogen column densities are in units of 10^{22} cm^{-2}.
[b] In units of erg s^{-1}. Values are not corrected for absorption. N/A: not applicable because of lack of spectral coverage.

Table 3. List of the 6.5 keV Fe emission line EWs, assuming a fixed line width of 0.1 keV, for the various X-ray observations covering that spectral energy. Errors and upper limits are at a 90% confidence level. Pointings are listed in chronological order from top to bottom.

Observation	*EW* (eV)
EXOSAT I	<56
EXOSAT II	<73
RXTE	48^{+13}_{-10}
BeppoSAX	51 ± 20
Swift	<1100

covering absorber and of an ionized absorber (as modeled by Balucińska-Church & McCammon 1992) was found acting on the Comptonization component. We also noted that the thermal component could be described with an optically thin hot diffuse gas (MEKAL; Mewe et al. 1985) at relatively low temperature ($kT_{\rm MEKAL} \sim 0.07$ keV); the thermal component could not be fitted with a blackbody or a disk-blackbody emission.

The spectral fit is slightly improved ($\Delta\chi^2 = 4$ for 2 d.o.f. less) by the addition of a narrow (with width σ fixed at 0.1 keV) Fe emission line at ∼6.5 keV. In order to estimate the significance of this line, we used the F-test statistics for the case of an additional component (e.g., Bevington 1969): we find that the line has a chance improvement probability of 1×10^{-3}. The *BeppoSAX* spectrum and the corresponding best fit model are reported in Fig. 3, upper left panel.

To further study the presence of the soft excess found in the *BeppoSAX* spectrum, we analyzed the 0.1−2 keV spectral data of the *ROSAT* observation. Due to the fact that the *ROSAT* spectrum has a smaller energy coverage and suffers from a lower S/N than the *BeppoSAX* one, we had to constrain the absorption and Comptonization component parameters to the *BeppoSAX* best-fit values in order to study the optically thin plasma emission with a reasonable degree of precision. We find that the results (Fig. 3, upper right panel) are consistent with those of *BeppoSAX*. It should be noted that an acceptable description of the spectrum (with χ^2/d.o.f. = 17.7/18) could also be achieved without adding the partially covering absorption column; the parameters describing the low-energy thermal emission are in this latter case practically the same as those of the model with the partial absorption and reported in Table 2.

The analysis of *RXTE*, *Swift* and *EXOSAT* spectra can instead allow one to monitor the behaviour of the Comptonization component and of the absorption column associated with it as a function of time and of X-ray luminosity of the source. Using the model that best fits the *BeppoSAX* data we thus tried to describe the spectra of 4U 1954+31 secured with these X-ray satellites. However, as they do not cover the low-energy extreme of the X-ray band covered with *BeppoSAX* (i.e., below ∼1−2 keV), they are insensitive to the presence of the MEKAL and to the Galactic line-of-sight hydrogen column. Thus, we modeled these spectra with an absorbed Comptonization model alone, and we fixed the Galactic $N_{\rm H}$ associated with the WABS component to the best-fit *BeppoSAX* value.

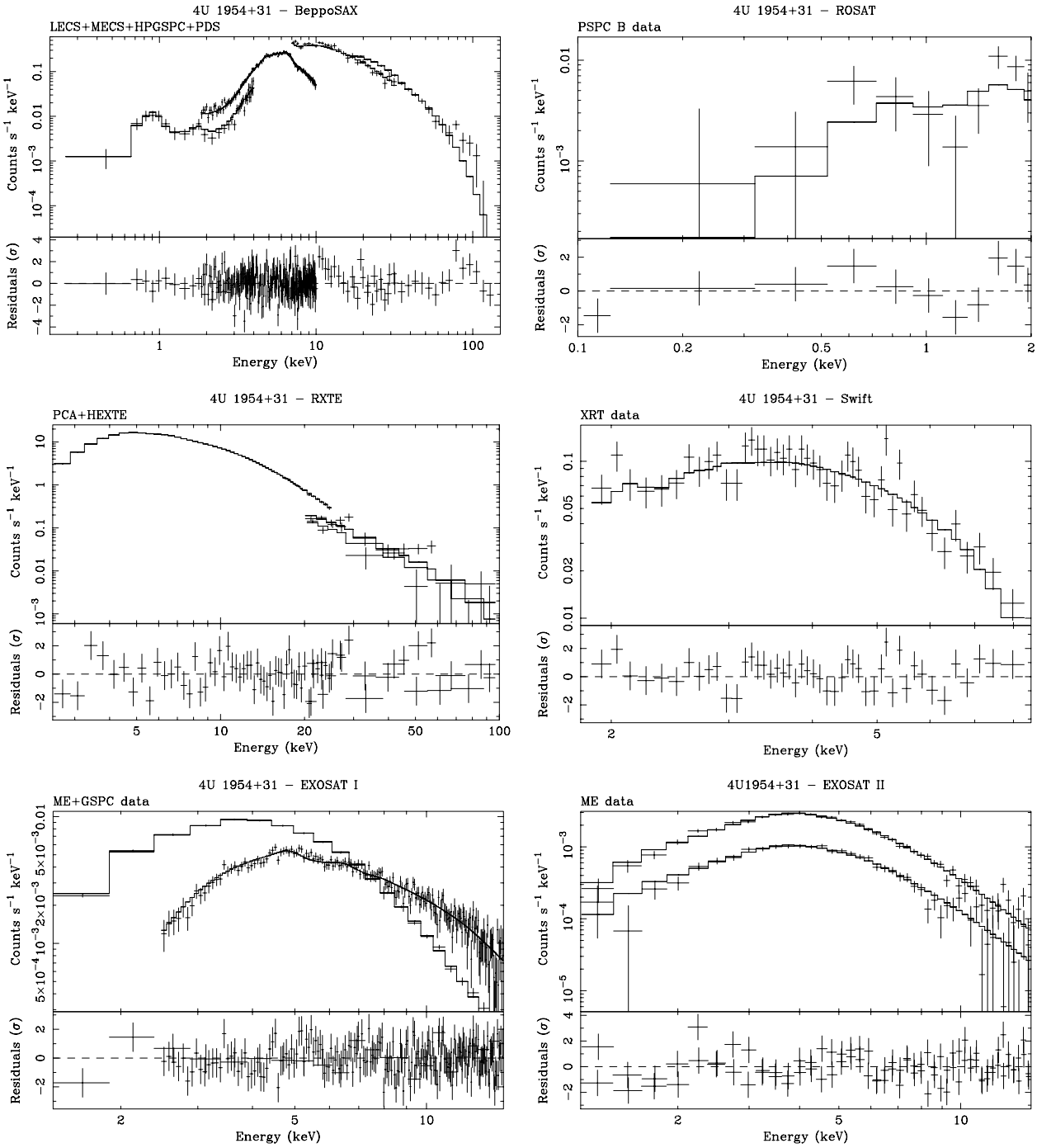

Fig. 3. X-ray spectra of 4U 1954+31 obtained from the pointed observations described in the text. The fit residuals using the best-fit model reported in Table 2 are also associated with each spectrum. (*Upper panels*) *BeppoSAX* LECS+MECS+HPGSPC+PDS (*left*) and *ROSAT* PSPC B (*right*) spectra. (*Central panels*) *RXTE* PCA+HEXTE (*left*) and *Swift* XRT (*right*) spectra. (*Lower panels*) spectra of *EXOSAT* observations I (ME+GSPC data; *left*) and II (ME data; *right*). For observation II, the spectra of the high and low states (first 5 ks and remaining part of the observation, respectively; see Fig. 2, upper right panel, for reference) are shown.

The *RXTE* PCA+HEXTE spectrum, reported in Fig. 3, central left panel, apparently does not need the presence of a partial convering absorption, and only a warm absorber is required. However, the fit is not formally acceptable (with χ^2/d.o.f. = 170.0/107) and shows large residuals around 6.5 keV. We therefore added a narrow emission line similar to that of the *BeppoSAX* best-fit model. This new description gives a $\Delta\chi^2 = 57.4$ for 2 d.o.f. less, meaning a chance improvement probability of 4×10^{-10} according to the F-test statistics. The best-fit parameter values of the Comptonization component as determined from the *RXTE* data are comparable to those measured from the *BeppoSAX* spectrum (see Table 2).

EXOSAT pointings caught 4U 1954+31 at different emission levels, with the source being on average six times brighter during observation I than in observation II. During both pointings, the spectral description does not need any absorption besides the Galactic one. It is found that, while observation II data give Comptonization values broadly similar to those of

the *BeppoSAX* observation (which was performed at a similar 2−10 keV source flux), observation I shows that 4U 1954+31 had a larger Compton cloud optical depth τ and smaller electron cloud and seed photon temperatures kT_{e^-} and kT_0. We also find that the addition of an emission line at 6.5 keV is not needed in the best-fit model for both observations, with EW upper limits slightly tighter than, but broadly consistent with, those obtained by Gottwald et al. (1995) from the same data. The spectra of the *EXOSAT* pointings are reported in the lower panels of Fig. 3.

Swift XRT data (Fig. 3, central right panel) span a smaller spectral range and have a lower S/N with respect to the *BeppoSAX*, *RXTE* and *EXOSAT* observations; nevertheless, the Comptonization model fits the *Swift* spectrum reasonably well, with parameter values (although affected by large errors) midway between those of the *BeppoSAX* and *EXOSAT* I best fits. The best-fit *Swift* spectrum does not need the presence of either an ionized absorber, or an iron emission line at 6.5 keV, and has a lower partially covering absorption column density with respect to the *BeppoSAX* observation.

We again explored the high-energy part of the *BeppoSAX* spectrum to look for the presence of a Cyclotron Resonant Feature (CRF) in absorption, which is considered one of the signatures of a highly magnetic NS hosted in an X-ray binary system (e.g., Orlandini & Dal Fiume 2001, and references therein). We used a CYCLABS multiplicative model (Mihara et al. 1990; Makishima et al. 1990), but it did not statistically improve the best-fit model of Table 2. Among the other pointings, thanks to its spectral coverage, only *RXTE* potentially allows one to perform a similar study. However, the lower S/N of HEXTE data did not allow us to explore the *RXTE* spectra.

As a further test of the presence of a CRF, we also performed a Crab ratio of the *BeppoSAX* PDS spectrum. This technique was used to successfully pinpoint CRFs in numerous X-ray binary pulsars (see, e.g., Orlandini et al. 1998), and consists of obtaining the ratio between the count rate spectrum of the source and that of the featureless power law spectrum of the Crab. This ratio has the advantage of minimizing the effects due to detector response, non-perfect modeling of the spectral continuum and calibration uncertainties. Any real feature present in the source spectrum can then be enhanced by multiplying the ratio by the functional form of the Crab spectrum (a power law with photon index $\Gamma = 2.1$) and by dividing it by the functional form of the continuum adopted to fit the broad-band source spectrum, obtaining the so-called Normalized Crab Ratio (NCR; see Orlandini et al. 1998 for details).

As a result, the NCR performed on the PDS spectrum of 4U 1954+31 further excludes the presence of any statistically significant absorption feature in the 15−150 keV range. This is at odds with the estimate of the magnetic field ($B \sim 10^{12}$ Gauss) of the NS hosted in this system made by Mattana et al. (2006), as it would produce a clear CRF around 25 keV. The 90% confidence level upper limit of the depth of any CRF at this energy is <0.25 assuming a feature width of 10 keV.

4. Discussion

The broadband, long-term X-ray study of 4U 1954+31 presented here, and performed through the analysis of data collected by five satellites, gave us the possibility to thoroughly study the long- and short-term high-energy behaviours of this bright but neglected source. In particular, with the widest ever broadband data coverage (0.2−150 keV) of this source, secured with *BeppoSAX* and shown here for the first time, we could characterize the X-ray spectrum of this object and check the best-fit model thus obtained against the observations acquired with *RXTE*, *ROSAT*, *EXOSAT* and *Swift*. Here we will discuss the results of the previous section and will compare them with the high energy behaviour of its twin, the symbiotic X-ray binary 4U 1700+24.

4.1. Broadband X-ray properties of 4U 1954+31

The temporal analysis of the light curves of the *RXTE* ASM and of the pointed observations confirms that the source has pronounced long- and short-term variability, but also that it does not show any periodicity on either small (seconds to tens of minutes) or large (days to years) timescales. In particular, we did not find evidence for the 5-h periodic signal detected by Corbet et al. (2006) and Mattana et al. (2006) in any of the satellite pointings. However, as can be seen from Fig. 2, this can be due to several factors: (a) the relatively short duration of the observations (in general lasting less than one single periodicity cycle); (b) the sparse light curve sampling; and (c) the presence of large flares throughout each pointing.

The presence of shot-noise stochastic variability (first found by Cook et al. 1984) is instead confirmed for the X-ray emission of 4U 1954+31, while no short-period hardness ratio variations are detected during each pointed observation. These "colorless" short-term fluctuations in the X-ray flux may be produced by instabilities in the accretion process, or by inhomogeneities in the velocity and/or density of an accreted stellar wind (or by both; e.g., Kaper et al. 1993). Thus, the observed random variability points to an explanation for this X-ray activity as due to an inhomogeneous accretion flow onto a compact object (e.g. van der Klis 1995).

The lack of evidence for X-ray eclipses in 4U 1954+31 suggests that either this system is viewed at a low (or intermediate) inclination angle, or that the orbital period is quite long (hundreds of days). In fact, a hint of variations of the order of 200−400 days is found in the secular ASM X-ray light curve.

Concerning the spectral properties of 4U 1954+31, one can see that the best-fit spectral model is typical of accreting systems hosting a NS (e.g., Paizis et al. 2006 and references therein). We cannot exclude the presence of a BH in this system; however, the temperatures associated with the Comptonization component are those generally seen in LMXBs with an accreting NS. The detection of a 5-h modulation (Corbet et al. 2006), interpreted as the spin of the accreting object, supports the accreting NS scenario.

The presence of a WD in accretion is basically ruled out in terms of both X-ray luminosity and spectral shape (de Martino et al. 2004; Suleimanov et al. 2005; Barlow et al. 2006). The X-ray emission from 4U 1954+31 is also much harder and stronger than that expected from the corona of a late-type giant star, this also being generally 4−5 orders of magnitude lower (Hünsch et al. 1998) than the one detected in the pointed observations presented here.

As the source X-ray luminosity increases, the emission from the object becomes harder. This is consistent with a model in which enhancement of accreting matter onto a compact object is responsible for the observed spectral shape and variability. In addition, the hardening of the spectrum with increasing luminosity seems to indicate accretion of matter with low specific angular momentum (i.e., from a wind), as suggested by e.g. Smith et al. (2002) and Wu et al. (2002) to explain a similar spectral behaviour observed in other X-ray binaries.

Comparison of X-ray spectral properties of the source among the different satellite pointings shows a trend in the

Comptonization parameters. In particular, an increase of τ and a decrease of kT_0 and kT_{e^-} is found when the 2−10 keV X-ray luminosity increases above 10^{35} erg s^{-1}. At this luminosity, the source possibly undergoes a spectral state change.

We found indications of complex and variable absorption around this X-ray source. A hint of this was already qualitatively suggested by Tweedy et al. (1989), although their narrower spectral coverage did not allow them to explore this behaviour in detail. Indeed, the upper limit to the interstellar Galactic absorption along the source line of sight is estimated as $N_{\rm H}^{\rm Gal} = 0.84{\times}10^{22}$ cm^{-2} (Dickey & Lockman 1990); from the *BeppoSAX* data we find that the line-of-sight hydrogen column is at least about a factor of two higher. The presence of a complex, variable and stratified neutral plus ionized absorbing medium may be explained by a NS accreting from a wind.

Complex absorbers are sometimes seen at energies less than 3 keV and can be described with a "two-zone" model (Haberl et al. 1989), where X-rays pass in series through a highly ionized absorber closer to the accretor and then a cold absorber farther away; 4U 1954+31 thus seems to belong to this source typology. This spectral behaviour is not unexpected from a source embedded in a stellar wind. In this sense, the detection of a relatively faint and narrow iron emission line suggests the presence of dense, ionized and radially infalling material in the close vicinity of the X-ray source.

Likewise, the nondetection of an accretion disk is explained by the low angular momentum of the accreted stellar wind, which then falls nearly directly onto the NS surface without forming a large accretion disk structure. If the NS is magnetized as suggested by the periodicity detected by Corbet et al. (2006), the accretion flow in the vicinity of the compact object is likely to be funneled onto the NS magnetic polar caps, thus leaving little room for the formation of a disk structure, albeit small.

Concerning the magnetic field strength of the NS hosted in 4U 1954+31 we note that the nondetection of a CRF from this source is not unexpected, as other long spin period NSs do not show unambiguous CRF signatures (e.g., 4U 0114+65; Masetti et al. 2006b). The absence of a detectable CRF also casts some doubt on the possibility that this system hosts a highly-magnetized ($B \sim 10^{12}$ Gauss) NS as suggested by Mattana et al. (2006).

A further indication that the accreting matter is flowing onto the NS polar caps via magnetic field confinement comes from the estimate of the size r_0 of the region emitting the Comptonization soft X-ray seed photons. Following the prescription by in't Zand et al. (1999) for the computation of r_0, and using the best-fit spectral parameters reported in Table 2, we obtain that $r_0 \sim 0.6$−1.6 km, depending on the Comptonization state of the source. This estimate suggests that the area emitting soft seed photons on the NS covers only a fraction of its surface and it is comparable with the size of the base of an accretion column, which is ≈0.1 times the NS radius (e.g., Hickox et al. 2004).

From the above spectral information, we propose a model for this system similar to that developed by Hickox et al. (2004) for HMXBs hosting a NS accreting from the stellar wind of the companion. These authors indeed found that a soft excess around 0.1 keV is a ubiquitous feature in the X-ray spectrum of HMXBs hosting a pulsating NS. Although the nature of the secondary is different in the case of 4U 1954+31, the proposed accretion mode (via dense stellar wind) is the same, therefore producing a similar behavior in the X-ray emission properties.

Hickox et al. (2004) suggest that, for sources with luminosity $L_{\rm X} \lesssim 10^{36}$ erg s^{-1} (see right panel of their Fig. 3), the NS is embedded in a diffuse cloud. The inner parts of this cloud may be ionized, absorb the blackbody radiation photons from the NS surface and upscatter part of them via Comptonization mechanism. The (much cooler) external parts of this cloud also emit thin thermal plasma radiation, by collisional energization or reprocessing of a fraction of the hard X-ray emission coming from the Comptonization region inside the cloud by the optically thin external layers. The cloud is also responsible for the overall two-zone variable absorption detected in X-rays.

In the light of all of these findings from our X-ray monitoring campaign, we conclude that 4U 1954+31 is a symbiotic X-ray binary in which a mildly magnetized NS is embedded in, and accreting from, a complex and variable stellar wind coming from the secondary star, an M-type giant.

4.2. Comparison with the system 4U 1700+24

We now draw a comparison between 4U 1954+31 and the other symbiotic X-ray binary 4U 1700+24.

In terms of time scale variations of the X-ray emission, both systems show fast shot-noise variations, indicating that they are both powered by accretion onto a compact object, most likely a NS although up to now no evidence of a variability associated with a spin period was found in 4U 1700+24 (see Masetti et al. 2002 for details and an interpretation thereof in terms of system geometry). Galloway et al. (2002) suggested that the spin non-detection may be due to the fact that the NS could be slowly rotating. If true, this would be a further similarity between the two systems.

Regarding the long-term variations, the behaviour seen in the ASM light curve of 4U 1954+31 is reminiscent of that shown by 4U 1700+24 and is interpreted as a modulation linked to the orbital motion of the system components (Masetti et al. 2002; Galloway et al. 2002). For 4U 1954+31, however, we did not find variations which are as periodic and stable as those found in 4U 1700+24 (although see Mattana et al. 2006 for the possible presence of a 385-day period in 4U 1954+31).

Spectral analysis of these two sources caught at different emission states shows that the Comptonization emission parameters of 4U 1954+31, when observed at low luminosity (few 10^{34} erg s^{-1} in the 2−10 keV band), are comparable to those shown by 4U 1700+24 during the phases of enhanced X-ray emission (when it reaches a similar X-ray luminosity, i.e., $\sim 10^{34}$ erg s^{-1}; Masetti et al. 2002). So it seems that the Comptonization emission mechanism in these two sources forms a continuum depending on the luminosity state, thus suggesting a comparable overall accretion mechanism for these two X-ray binaries.

The relatively high luminosity of 4U 1954+31, when compared to 4U 1700+24 (which is on average at luminosities which are 1−2 orders of magnitude fainter; Masetti et al. 2002), may indicate an intense stellar wind activity or, more likely, that the NS orbits much closer to the M-type giant than in the 4U 1700+24 case. This would also explain the greater absorption in the accreting flow, as in this way the NS hosted in 4U 1954+31 would move into a denser medium.

4U 1954+31, differently from 4U 1700+24, does not show the presence of blackbody emission from the accreting NS in its X-ray spectrum. This is reasonably explained by the fact that the former source shows the presence of a complex (and possibly variable) absorption around the X-ray emitter, which either absorbs the direct NS surface emission (at lower X-ray luminosities, when the accretion flow appears to be denser) or upscatters it via Comptonization processes (during the higher X-ray

luminosity states, when the Compton cloud has a greater optical depth τ).

The two systems may however show a similar behaviour concerning the soft X-ray excess detected in both of them. Indeed, Tiengo et al. (2005) found in the *XMM-Newton* spectrum of 4U 1700+24 an excess which they modeled with a wide Gaussian line centered on 0.5 keV. A similar feature is present in the *BeppoSAX* spectrum of 4U 1954+31 presented here, and which we modeled as an optically thin plasma emission. It may thus be possible that the soft excess seen in 4U 1700+24 can be modeled in the same way.

The absence of emission lines (or more generally of features connected with the accretion process) in the spectrum of the optical counterpart of 4U 1954+31 (Masetti et al. 2006a), as in the case of 4U 1700+24, is naturally explained by the comparison between the X-ray luminosity of 4U 1954+31 ($\approx 10^{35}$ erg s^{-1}; see Table 2) and the total luminosity of its M-type giant companion, ~900 $L_{\odot}$ (Lang 1992), i.e. 3.4×10^{36} erg s^{-1}, for a M4 III star (Masetti et al. 2006a). As most of the luminosity of the M-type giant is emitted in the optical and near-infrared bands, it can be understood that X-ray irradiation has little effect on the secondary star.

We speculate that the 4U 1954+31 system evolution is halfway between that of 4U 1700+24, where the compact object is accreting from a wind with lower density (probably because it is orbiting farther away from the secondary), and GX 1+4, where a high accretion rate onto the NS is apparent from X-ray and optical data (Chakrabarty & Roche 1997) implying that the latter system is tighter (with the secondary filling its Roche lobe, thus producing an accretion disk around the compact object) than 4U 1700+24 and 4U 1954+31.

5. Conclusions

We have presented a broadband multi-spacecraft analysis of the symbiotic X-ray binary 4U 1954+31. This allowed us, for the first time, to explore in detail the X-ray characteristics of this "forgotten" source. From the timing analysis we found that, while random X-ray variability is present on long and short time scales, no periodic modulation is found. X-ray spectroscopy shows that the high-energy photons radiated from this source are produced by Comptonization plus thin thermal plasma emission. These two components, in particular the Comptonization, suffer from complex variable absorption, likely originating in the accretion flow itself. An iron emission line is also possibly detected.

From the interpretation of the above data and from the comparison with similar sources, the scenario that we envisage is that of a mildly magnetized NS orbiting around an M-type giant and accreting matter from the companion star stellar wind, which is inhomogeneous in terms of density and ionization degree, with the inner parts of the radial accretion flow possibly ionized by the NS high-energy radiation. We thus conclude that 4U 1954+31 is a symbiotic LMXB which has several of the characteristics, in terms of accretion structure, usually found in HMXBs. This likely led earlier studies to the conclusion (from the X-ray data analysis alone) that this source is an HMXB; only recently, thanks to combined optical and X-ray observations, was it found that 4U 1954+31 is actually an LMXB (Masetti et al. 2006a).

The soft excess observed in the X-ray spectrum of 4U 1954+31 may be in the form of a group of discrete X-ray emission lines produced by light metals, rather than a continuum emission. This is suggested by the fact that this excess is modeled with an optically thin thermal plasma model. Unfortunately, the relatively low spectral resolution of the data considered in this paper does not allow us to better explore this issue. Detailed modeling is needed to understand the nature of the observed complex spectral shape below 2 keV. To this aim, high-resolution spectroscopy with *XMM-Newton* or *Chandra* is, at present, the optimal choice.

Acknowledgements. BeppoSAX was a joint program of ASI and of the Netherlands Agency for Aerospace Programs (NIVR). This research has made wide use of data obtained through the High Energy Astrophysics Science Archive Research Center Online Service, provided by the NASA/Goddard Space Flight Center. This research has also made use of the SIMBAD database, operated at CDS, Strasbourg, France and of the ASI Space Data Center *Swift* archive. ASM data were provided by the *RXTE* ASM teams at MIT and at the *RXTE* SOF and GOF at NASA's GSFC. This work was partially supported through ASI/INAF grant No. I/023/05/0. We thank the anonymous referee for useful comments.

References

Arnaud, K. A. 1996, XSPEC: the first ten years, in Astronomical Data Analysis Software and Systems V, ed. G. H. Jacoby, & J. Barnes, ASP Conf. Ser., 101, 17
Balucińska-Church, M., & McCammon, D. 1992, ApJ, 400, 699
Barlow, E. J., Knigge, C., Bird, A. J., et al. 2006, MNRAS, 372, 224
Baskill, D. S., Wheatley, P. J., & Osborne, J. P. 2006, MNRAS, 357, 626
Bevington, P. R. 1969, Data reduction and error analysis for the physical sciences (New York: McGraw-Hill Book Company)
Blackburn, J. K. 1995, FTOOLS: A FITS Data Processing and Analysis Software Package, in Astronomical Data Analysis Software and Systems IV, ed. R. A. Shaw, H. E. Payne, & J. J. E. Hayes, ASP Conf. Ser., 77, 367
Boella, G., Butler, R. C., Perola, G. C., et al. 1997a, A&AS, 122, 299
Boella, G., Chiappetti, L., Conti, G., et al. 1997b, A&AS, 122, 327
Buccheri, R., Bennett, K., Bignami, G. F., et al. 1983, A&A, 128, 245
Burrows, D. N., Hill, J. E., Nousek, J. A., et al. 2005, Space Sci. Rev., 120, 165
Bradt, H. V., Rothschild, R. E., & Swank, J. H. 1993, A&AS, 97, 355
Chakrabarty, D., & Roche, P. 1997, ApJ, 489, 254
Chiappetti, L., & Dal Fiume, D. 1997, The XAS Data Analysis System, in Data Analysis in Astronomy, Proceedings of the Fifth Workshop ed. V. di Gesù, M. J. B. Duff, A. Heck, M. C. Maccarone, L. Scarsi, & H. U. Zimmerman (Singapore: World Scientific Press), 101
Cook, M. C., Warwick, R. S., & Watson, M. G. 1984, EXOSAT obsevations of 3A1954+319, in X-ray Astronomy '84, ed. M. Oda, & R. Giacconi, Institute of Space and Astronautical Science, 225
Corbet, R. H. D., Barbier, L., Barthelmy, S., et al. 2006, ATel, 797
de Martino, D., Matt, G., Belloni, T., Haberl, F., & Mukai, K. 2004, A&A, 415, 1009
Dickey, J. M., & Lockman, F. J. 1990, ARA&A, 28, 215
Fiore, F., Guainazzi, M., & Grandi, P. 1999, Technical Report 1.2, *BeppoSAX* scientific data center, available online at: `ftp://ftp.asdc.asi.it/pub/sax/doc/software_docs/saxabc_v1.2.ps`
Forman, W., Jones, C., Cominsky, L., et al. 1978, ApJS, 38, 357
Frontera, F., Costa, E., Dal Fiume, D., et al. 1997, A&AS, 122, 357
Galloway, D. K., Sokoloski, J. L., & Kenyon, S. J. 2002, ApJ, 580, 1065
Gehrels, N., Chincarini, G., Giommi, P., et al. 2004, ApJ, 611, 1005
Gottwald, M., Parmar, A. N., Reynolds, A. P., et al. 1995, A&AS, 109, 9
Haberl, F., White, N. E., & Kallman, T. R. 1989, ApJ, 343, 409
Hickox, R. C., Narayan, R., & Kallman, T. R. 2004, ApJ, 614, 881
Hünsch, M., Schmitt, J. H. M. M., Schröeder, K.-P., & Zickgraf, F.-J. 1998, A&A, 330, 225
in't Zand, J. J. M., Verbunt, F., Strohmayer, T. E., et al. 1999, A&A, 345, 100
Jahoda, K., Swank, J. H., Giles, A. B., et al. 1996, In-orbit performance and calibration of the Rossi X-ray Timing Explorer (*RXTE*) Proportional Counter Array (PCA), in EUV, X-ray and Gamma-ray Instrumentation for Space Astronomy VII, ed. O. H. Siegmund, & M. A. Gummin, Proc. SPIE, 2808, 59
Kaper, L., Hammerschlag-Hensberge, G., & van Loon, J. T. 1993, A&A, 279, 485
Lammers, U. 1997, The SAX/LECS Data Analysis System User Manual, SAX/LEDA/0010
Levine, A. M., Bradt, H. V., Cui, W., et al. 1996, ApJ, 469, L33

Liu, Q. Z., van Paradijs, J., & van den Heuvel, E. P. J. 2001, A&A, 368, 1021
Makishima, K., Mihara, T., Ishida, M., et al. 1990, ApJ, 365, L59
Manzo, G., Giarrusso, S., Santangelo, A., et al. 1997, A&AS, 122, 341
Masetti, N., Dal Fiume, D., Cusumano, G., et al. 2002, A&A, 382, 104
Masetti, N., Orlandini, M., Palazzi, E., Amati, L., & Frontera, F. 2006a, A&A, 453, 295
Masetti, N., Orlandini, M., Dal Fiume, D., et al. 2006b, A&A, 445, 653
Mattana, F., Götz, D., Falanga, M., et al. 2006, A&A, 460, L1
Mewe, R., Groenschild, E. H. B. M., & van den Oord, G. H. J. 1985, A&AS, 62, 197
Mihara, T., Makishima, K., Ohashi, T., Sakao, T., & Tashiro, M. 1990, Nature, 346, 250
Moretti, A., Perri, M., Capalbi, M., et al. 2006, A&A, 448, L9
Morrison, R., & McCammon, D. 1983, ApJ, 270, 119
Orlandini, M., Dal Fiume, D., Frontera, F., et al. 1998, A&A, 332, 121
Orlandini, M., & Dal Fiume, D. 2001, Hard X-ray tails and cyclotron features in X-ray pulsars, in: X-ray astronomy, ed. N. E. White, G. Malaguti, & G. G. C. Palumbo, AIP Conf. Proc. (Melville, NY: AIP), 599, 283
Paizis, A., Farinelli, R., Titarchuk, L., et al. 2006, A&A, 459, 187
Paltani, S., Attie, D., Domingo Garau, A., et al. 2006, ATel, 796
Parmar, A. N., Martin, D. D. E., Bavdaz, M., et al. 1997, A&AS, 122, 309
Peacock, A., Andresen, R. D., Manzo, G., et al. 1981, Space Sci. Rev., 30, 525
Pfeffermann, E., & Briel, U. G. 1986, Performance of the position sensitive proportional counter of the ROSAT telescope, in X-ray instrumentation in astronomy, Proc. SPIE, 597, 208
Romano, P., Campana, S., Chincarini, G., et al. 2006, A&A, 456, 917
Rothschild, R. E., Blanco, P. R., Gruber, D. E., et al. 1998, ApJ, 496, 538
Smith, D. M., Heindl, W. A., & Swank, J. H. 2002, ApJ, 569, 362
Suleimanov, V., Revnivtsev, M., & Ritter, H. 2005, A&A, 435, 191
Tiengo, A., Galloway, D. K., Di Salvo, T., et al. 2005, A&A, 441, 283
Titarchuk, L. 1994, ApJ, 434, 570
Tweedy, R. W., Warwick, R. S., & Remillard, R. 1989, 3A1954+319: a possible supergiant X-ray binary?, in 23rd ESLAB Symposium on Two Topics in X-Ray Astronomy. Volume 1: X-Ray Binaries, ed. J. Hunt, & B. Battrick, ESA Publications Division, SP–296, 661
Trümper, J. 1982, Adv. Space Res., 2, 241
Turner, M. J. L., Smith, A., & Zimmermann, H. U. 1981, Space Sci. Rev., 30, 513
van der Klis, M. 1995, in X-ray Binaries, ed. W. H. G. Lewin, J. van Paradijs, & E. P. J. van den Heuvel (Cambridge: Cambridge Univ. Press), 252
van Paradijs, J., & McClintock, J. E. 1995, in X-ray Binaries, ed. W. H. G. Lewin, J. van Paradijs, & E. P. J. van den Heuvel (Cambridge: Cambridge Univ. Press), 58
Voges, W., Aschenbach, B., Boller, T., et al. 1999, A&A, 349, 389
Voges, W., Aschenbach, B., Boller, T., et al. 2000, IAU Circ., 7432
Warwick, R. S., Marshall, N., Fraser, G. W., et al. 1981, MNRAS, 197, 865
White, N. E., & Peacock, A. 1988, Mem. Soc. Astron. It., 59, 7
White, N. E., Nagase, F., & Parmar, A. N. 1995, The properties of X-ray binaries, in X-ray Binaries, ed. W. H. G. Lewin, J. van Paradijs, & E. P. J. van den Heuvel (Cambridge: Cambridge Univ. Press), 1
Wu, K., Soria, R., Campbell-Wilson, D., et al. 2002, ApJ, 565, 1161

Online Material

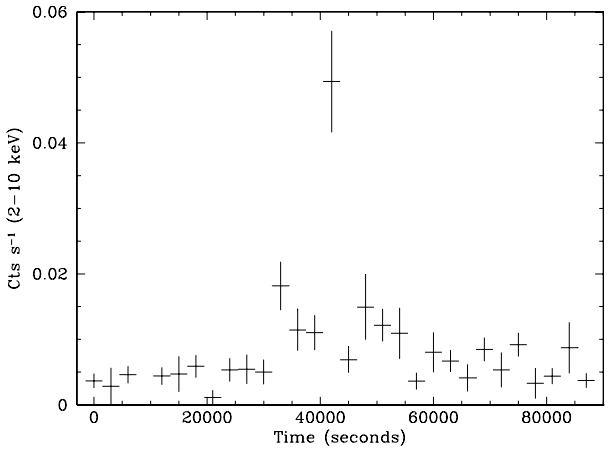

Fig. A.1. MECS 2−10 keV countrate light curve of the source EY Cyg.

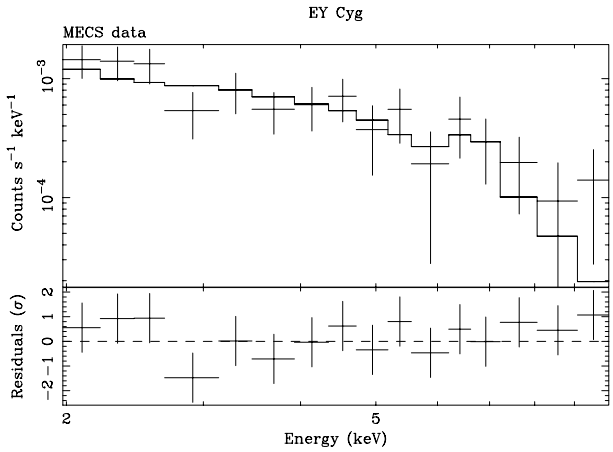

Fig. A.2. MECS 2−10 keV spectrum of the source EY Cyg, averaged over the *BeppoSAX* observation. Data (in the upper panel) are well fitted using a single-temperature optically thin thermal plasma model with $kT \sim 8$ keV. In the lower panel, the best-fit residuals are shown.

Appendix A: The X-ray emission from the field source EY Cyg

As explained in Sect. 2.1, the Cataclysmic Variable EY Cyg is present in the MECS field as a faint X-ray source. In order to check for any possible contamination from this object in the HPGSPC and PDS data, we extracted and analyzed the available information on EY Cyg as observed by the *BeppoSAX* MECS. Data were extracted from a region of 3′ centered on the source; their reduction was similar to that applied in Sect. 2.1 to the 4U 1954+31 MECS data, with the difference that, for the spectral analysis, we used the appropriate ancillary response function and background data for off-axis observations.

The 2−10 keV light curve during the entire *BeppoSAX* observation showed that EY Cyg had a steady behaviour, with a possible flare at half of the observation and lasting less than one hour (see Fig. A.1). The 5−10 keV / 2−5 keV hardness ratio of the source does not show significant variations during the *BeppoSAX* pointing: we therefore considered the 2−10 keV spectrum averaged over the entire observation.

Following the approach in Baskill et al. (2005), we fit the MECS spectral data using an absorbed optically thin thermal plasma (MEKAL model in XSPEC; Mewe et al. 1985). As no spectral information was available below 2 keV in the MECS data, we fixed the hydrogen column density to the value found by Baskill et al. (2005), i.e. 2.8×10^{21} cm^{-2}. The averaged spectrum was thus satisfactorily fitted (χ^2/d.o.f. = 8.3/14) with a $kT = 8^{+72}_{-4}$ (see Fig. A.2), in broad agreement with the results of Baskill et al. (2005). The best-fit model implied 7−30 keV and 15−150 keV fluxes for the EY Cyg emission in the HPGSPC and PDS ranges as shown in Table A.1.

Table A.1. Comparison of the X-ray fluxes (expressed in erg cm^{-2} s^{-1}) of EY Cyg and 4U 1954+31 in the 7−30 keV and in the 15−150 keV bands, together with their percentage ratio, as measured during the *BeppoSAX* pointing described in Sect. 2.1.

Spectral range (keV)	EY Cyg	4U 1954+31	Ratio (%)
7−30	5.5×10^{-13}	4.1×10^{-10}	0.13
15−150	1.5×10^{-13}	3.8×10^{-10}	0.039

As one can see from this Table, the comparison between the fluxes of 4U 1954+31 and EY Cyg indicates that any contamination from this field source on the spectrum of 4U 1954+31 is negligible.